REVIEWED

Entrainment of free water into hydraulic systems through the rod sealing

Tobias Mielke*, Katharina Schmitz* and Hubertus Murrenhoff*

RWTH Aachen University, Institute for Fluid Power Drives and Systems (IFAS),
Campus Boulevard 30, D-52074 Aachen, Germany*
E-Mail: Tobias.Mielke@ifas.rwth-aachen.de

Water in oil-based hydraulic systems is a source for many machinery failures. It accounts for up to 20% of the life expectancy failures and even before that, it impacts the expected performance negatively /1/. Water can enter a hydraulic system in various ways. In this article, the entry through the dynamic seal of the rod is investigated. After a brief description of the damage mechanisms of water in a hydraulic system, the theory of the entrainment is explained. The test bench is then described to study the effect. Finally, entrainment results for two test fluids (oil and water) are presented and compared to the theory.

Keywords: Rod Sealing, Water, Contamination, Reynolds Equation
Target audience: Science Community, Sealing manufactures

1 Damage in hydraulic systems by water

This section gives an overview of the damaging mechanisms of water in hydraulic systems. In addition to the damage to the pressure medium, the used components, made from different materials, are impacted by water.

1.1 Pressure medium ageing

The ageing process of pressure media used in hydraulics in presence of water occurs due to two mechanisms: oxidation, which occurs in mineral oil based fluids and hydrolysis, which takes place in ester based fluids. The effect of water plays the role of a catalyst and accelerates the process. Due to their relatively high electronegativity, oxygen ions can dissociate a hydrogen atom from a hydrocarbon molecule. This produces a hydrocarbon radical that forms a hydrocarbon peroxide radical with an oxygen atom. This is very reactive and attacks other molecules. The further elimination of a hydrogen atom results in a hydrocarbon hydroperoxide and a new hydrocarbyl radical. The formation of more and more radicals keeps the chain reaction going on resulting in products such as alcohols, aldehydes, ketones and acids.

The process of hydrolysis is displayed in Figure 1.

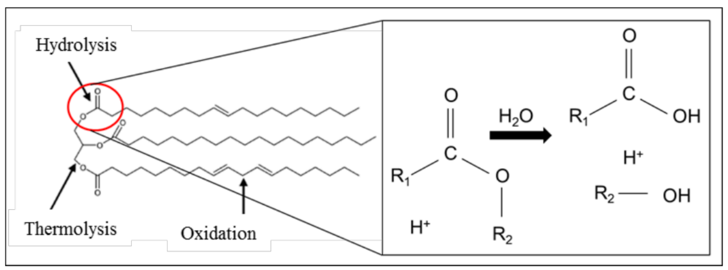

Figure 1: Hydrolysis on a 3-fold ester /2/, /3/

The two-valued alcohol group (shown on the left, encircled) has only a low hydrolytic stability. Water dissolves this site and forms an alcohol. The separated molecule residue becomes an acid (in the picture on the right). As a result, acidification of the system can occur, due to which metallic components can be corrosively attacked.

1.2 Seal Damage

Seals in hydraulic systems, which have the task of preventing leakage, come into direct contact with the fluid and react with it, so they can be attacked by the oil´s water contamination /4/. In /4/ the influence of water in oil on weight change of polyamide sealing elements after a defined time under the influence of different oil types and various humidity ranges is investigated. It is shown that with dry oil (0% water content), the sealing elements lose weight. Since at higher content levels water diffuses out of the oil into the sealing material, a weight gain is observed. That could squeeze the seal out of its installation grove and is commonly known as gap extrusion.

1.3 Damage to metallic components

In /4/ the influence of water on metallic components with regard to corrosion is investigated. There is a risk of corrosion particularly at locations where water can settle, for example at the bottom of the vessel. In valves or in narrow sealing gaps (e.g., in axial piston pumps) there is the risk that corrosion products lead to a clamping of the components and thus to dangerous or at least unwanted behaviour of the system.

2 Theory of Blok

The sealing mechanism of rod seals is commonly described by Blok's theory /5/. On the basis of this theory, fluid can be entrained into the hydraulic system via the rod seal. The basics and the resulting entrainment mechanism are explained below.

In the case of dynamic seals, a fluid-filled sealing gap (gap height h usually <1 µm) is formed between rod and seal. The pressure distribution in the fluid gap corresponds to the previous pressing in the gap, due to the preloading of the seal during assembly and the system pressure. The mechanism of returning the fluid is called dynamic sealing. The calculation of rod seals is based on the "inverse-Reynolds theory". Rod seals are dynamically sealed when the oil volume being pulled out during the extension of the cylinder is smaller than the oil volume that could theoretically be dragged back into the cylinder during retraction. The drag volume depends on the rod diameter and the lubricant film height. For the purpose of designing rod seals, the lubrication film heights for inward and outward travel are calculated and compared. For dynamic tightness, the theoretical retraction film height must be larger than the extension film height.

The Reynolds equation, applied to the gap between seal and rod, takes the form as given in Equation (1). It couples the spatial pressure gradient $\frac{\partial p}{\partial x}$ with the viscosity η, the rod velocity u and the gap height h. $h_a{}^*$ is the lubricating film height at the point of the pressure maximum at which the spatial gradient equals zero.

$$h^3 \cdot \frac{\partial p}{\partial x} - 6 \cdot \eta \cdot u_a \cdot (h - h_a{}^*) = 0 \quad (1)$$

Rod seals are pressed against the rod by the preload and the applied system pressure when the system is not moving. The resulting stress is supported by the lubrication film on the rod via the fluid pressure. Furthermore, the pressure in the lubrication film normal to the piston rod is assumed to be constant /5/, /6/. For the calculation of the lubricating film thickness, therefore, the fluid pressure is equated with the stress distribution previously determined by experiments or FEM calculations. A typical pressure profile as well as the velocity distribution in the lubrication gap is shown in Figure 1.

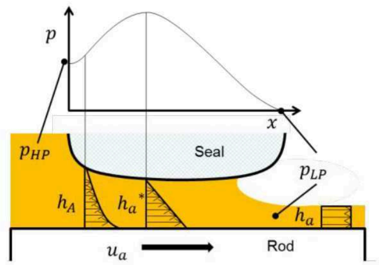

Figure 2: Pressure and velocity distribution underneath the seal lip

The system pressure p_{HP} is applied to one side of the seal. Due to the geometry of the sealing element, the pressure rises very steeply (steeper than shown in the figure, since otherwise the relevant points could not be represented). When a maximum is reached, the pressure drops to ambient pressure p_{LP}. The pressure increase prevents leakage of the fluid. The best sealing is obtained with a triangular pressure profile with the maximum near to the sealed region.

To determine the film height on the rod h_a, Equation (1) is derived with respect to x (Equation (2)).

$$h^3 \frac{\partial^2 p}{\partial x^2} + \frac{\partial h}{\partial x}\left(3h^2 \frac{\partial p}{\partial x} - 6\eta u_a\right) = 0 \tag{2}$$

In an inflection point of the pressure distribution (where the greatest change in pressure is observed) the first term of the left side of the equation equals 0. To fulfill the equation the difference in the brackets has to equal 0 as well. Rearranging the equation reveals the gap height underneath the inflection point of the pressure distribution (Equation (3)).

$$h_A = \sqrt{2\eta \frac{u_a}{\left(\frac{\partial p}{\partial x}\right)_A}} \tag{3}$$

Inserting h_A back into Equation (1) and evaluating it at the same spot delivers the gap height $h_a{}^*$ underneath the maximum of the pressure distribution where the pressure driven fluid velocity is 0 and its distribution therefore linear (Equation (4)).

$$h_a{}^* = \sqrt{\frac{8}{9}\eta \frac{u_a}{\left(\frac{\partial p}{\partial x}\right)_A}} \tag{4}$$

Assuming that the volume remains constant, h_a on the rod can easily be derived by applying volume consistency (Equation (5)).

$$h_a = \frac{1}{2} h_a{}^* = \sqrt{\frac{2}{9}\eta \frac{u_a}{\left(\frac{\partial p}{\partial x}\right)_A}} \tag{5}$$

The entrainment potential can be quantified as a difference volume between retraction and extension based on the presented mechanism. This is calculated according to Equation (6). Index a and A stand for outward travel, e and E for inward, the same theory applies to both directions.

$$\Delta V = \pi d H \sqrt{\frac{2\eta}{9}} \cdot \left(\sqrt{\frac{u_e}{\left(\frac{\partial p}{\partial x}\right)_E}} - \sqrt{\frac{u_a}{\left(\frac{\partial p}{\partial x}\right)_A}} \right) \tag{6}$$

If ΔV is equal to or greater than 0, which means that more volume can be entrained through the seal than travels out before, the sealing is called tight.

When fluid is applied to the outside of the seal, e.g. water on the rod, it can be entrained when the rod is retracted. This is particularly problematic in mobile hydraulic machines, which are also operated under rain and partly under water.

Water has a different viscosity than hydraulic oil and will therefore be dragged differently. The ratio of the entrained volumes, assuming that the pressure distribution and the speed of the rod remains the same, is given in Equation (7). It is furthermore assumed, that the absolute oil film height during extension is negligible compared to the water film height during entrainment.

$$\frac{\Delta V_{Water}}{\Delta V_{Oil}} = \sqrt{\frac{\eta_{Water}}{\eta_{Oil}}} \tag{7}$$

A similar ratio is found in /7/.

Using literature data for viscosity of water and oil at different temperatures, the expected relation can be plotted as shown in Figure 3.

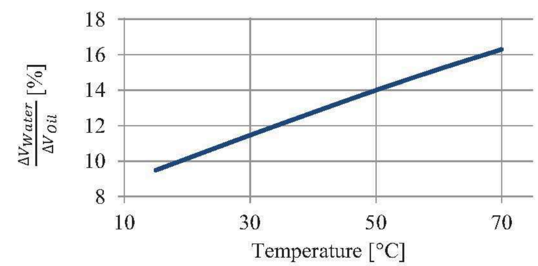

Figure 3: Expected relation for entrained water vs. entrained oil

For an average temperature range of hydraulic systems, the relation ranges from 10% up to 16.5%.

The theory given is only valid if the oil layer, which adheres to the rod when it is extended; remains adhered to it during the entire time. When supplied with water, it will lie on top of the oil film with no influence on it.

3 Test bench

In this section, the developed test bench to measure entrained water through the rod seal is presented. Furthermore, a proof of concept of the system is conducted.

3.1 Test chamber

At the Institute for Fluid Power Drives and Controls (IFAS), a test bench was set up to investigate the entrainment of free water. The test bench is shown in Figure 4.

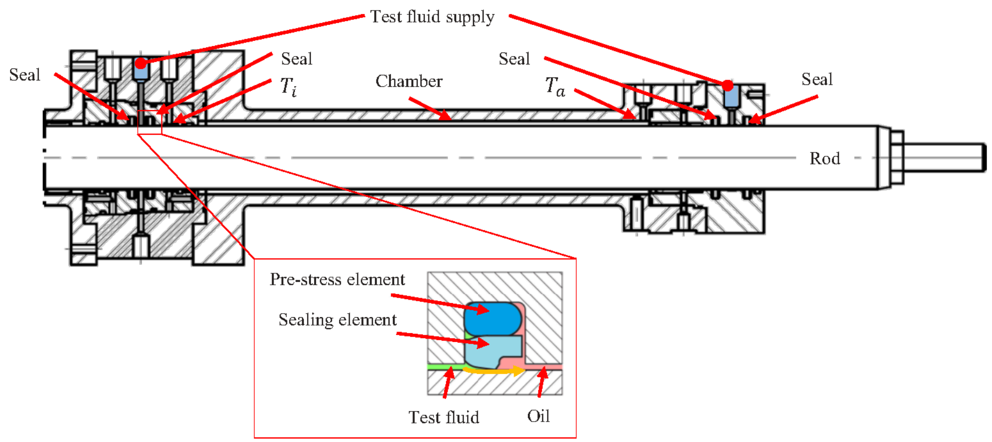

Figure 4: Test bench concept and design

A hollow piston rod, which oscillates with a maximum stroke of 350 mm during the tests, passes through a chamber, which is closed on both sides with seals. The outside of the seals is supplied with test fluid (oil or water). The chamber is filled with HLP 46 oil. The relatively short test fluid supply chamber is sealed to the outside with another seal.

An O-ring made of NBR is used as a pre-stress element. A starting effect is inherent for this type of seals /8/. This is considered completed, since the seals have run at least 2100 m before the tests.

Through operation, fluid volume ΔV from the outside is entrained into the chamber. To control the temperature a coolant is directed through the bore of the rod. Furthermore, two temperature sensors (T_i and T_a) are installed to monitor the oil temperature in front of the respective seals.

3.2 Entrainment Sensor

The entrained volume is measured with a self-developed sensor which is shown in Figure 5. The hydraulic part is drawn in greater detail to show relevant components (red box).

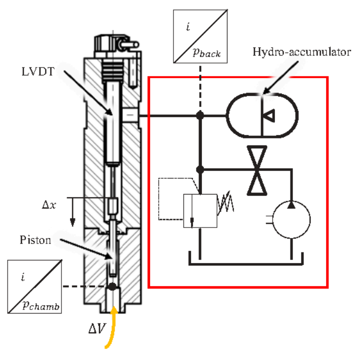

Figure 5: Entrainment sensor

It consists of a piston, which is sealed by a rod seal. The space in front of the piston is connected to the chamber. A LVDT is attached to the piston measuring the displacement. Entrained water volume ΔV displaces the piston and can be calculated with the piston diameter. In order to maintain a constant pressure p_{chamb} in the chamber, pressure p_{back} is applied to the reverse side of the piston. This pressure is provided by a 4-liter hydro-accumulator, which is almost completely empty. The displaced volume of the piston is taken up into the accumulator and the pressure remains constant during operation.

3.2.1 Validation of the pressure dependency

In order to verify the suitability of the measuring system, the relationship between chamber pressure and displacement of the piston was checked. The theoretical relation is given in Equation (8) /9/.

$$\Delta p = \frac{E'_{Fl}}{V_0} \cdot \Delta V_i = \frac{E'_{Fl}}{V_0} \cdot A \cdot \Delta x \tag{8}$$

Δp is the pressure rise due to an additional volume ΔV which is squeezed into the original volume V_0. E'_{Fl} is the corrected bulk modulus of the fluid. In this case ΔV can be calculated as a function of the displacement Δx of the piston and its cross sectional area A. V_0 and E'_{Fl} are considered constant which leads to a linear relation between Δx and Δp. Water has a negligible influence on the bulk modulus as it is only present in small fractions (see Figure 3) and its immiscibility with oil.

The piston is displaced by increasing the pressure on the back thus the resulting pressure in the chamber along with the actual displacement of the piston are measured. The results are shown in Figure 6.

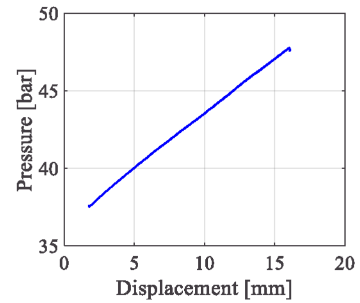

Figure 6: Measured relation between piston displacement and chamber pressure

As shown in the Figure there is a good linearity between piston displacement and chamber pressure. In addition the constancy of back pressure in respect to piston displacement was evaluated.

Figure 7 shows the pressure p_{back} while displacing the piston, which leads to a volume flow into the accumulator. It can be seen that the back pressure remains constant.

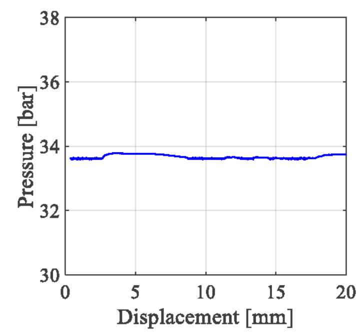

Figure 7: Pressure in accumulator while displacing piston

Both results, the linearity between piston displacement and chamber pressure as well as the constant back pressure, lead to the conclusion, that the entrainment sensor is well suited for the purpose.

3.3 Temperature dependency

During tests, an increase in oil temperature may occur due to the change in ambient temperature, frictional heat or other circumstances. As a result, the oil expands and, especially in the present case, this would lead to a movement of the piston and thus falsify the measurement results. In the following section, the temperature-dependent displacement effect of the sensor´s piston is explained. Then a method is presented which is used to neglect the effect due to recalculation. Finally, the results of the heating measurement which are necessary for the parameterisation of the method are presented. This is done when the rod is at a standstill.

3.3.1 Temperature induced expansion of volume

With a rise in temperature most materials expand their geometric dimension. For liquids, this effect is expressed in an increase of volume. In the present case, this would lead to a displacement of the piston and would thus falsify the measurement results.

In order to calculate this effect, measurements in dependency of temperature were carried out. The temperature is increased slowly, and the displacement of the piston is recorded. In the experiments, the temperature-dependent displacement can thus be subtracted from the measurement signal, and the entrained volume can be determined according to Equation (9).

$$\Delta V_{entrained} = \Delta V_{measured} - \Delta V_{therm} = A_{piston} \cdot (\Delta x_{measured} - \Delta x_{therm}) \tag{9}$$

A_{piston}represents the cross sectional area of the piston and Δx_i the displacement of the piston (measured and due to thermal effects). It is assumed, that the inside volume of the chamber remains constant during testing and that only the volume expands. As the chamber system is closed and state of the art sealing is applied, it is furthermore assumed, that the oil mass in the chamber remains constant.

According to /9/ the change in volume of a mineral oil ΔV can be calculated using Equation (10).

$$\Delta V_{therm} = V_0 \cdot \gamma \cdot \theta = A_{piston} \cdot \Delta x_{therm} \tag{10}$$

V_0 is the original Volume, γ the expansion coefficient (here $7 \cdot 10^{-4} K^{-1}$ /9/) and θ the deviation of the temperature from a reference temperature. Rearranging of Equation (10) gives a relation between an increase in temperature and the resulting displacement (Equation (11)).

$$\frac{V_0 \cdot \gamma}{A_{piston}} \cdot \theta = \Delta x_{therm} \tag{11}$$

Derivation of Equation (11) yields the displacement gradient with respect to the temperature.

Furthermore Equation (12) applies:

$$\theta = T - T_{ref} \rightarrow \frac{dx}{d\theta} = \frac{dx}{dT} \tag{12}$$

Putting the design (given in Table 1) and fluid parameters into this Equation the numerical relation between $\Delta\theta$ and Δx_{therm} is derived (Equation (13)).

V_0	220921.7 mm³
A	28.27 mm²

Table 1: Test bench design parameters

$$5.47 \frac{mm}{K} \cdot \Delta\theta = \Delta x_{therm} \tag{13}$$

This means that an increase in temperature of 1 K will theoretically result in a displacement of 5.47 mm of the piston.

Piston displacement due to a temperature change can be compensated by measuring the temperature of the fluid, calculating the resulting change and subtracting it from the measured displacement $\Delta x_{measured}$ (Equation (14)).

$$\Delta x_{therm} = \Delta x_{measured} - \Delta x_{therm} = \Delta x_{measured} - 5.47 \frac{mm}{K} \cdot \Delta\theta \tag{14}$$

3.3.2 Heating tests

To verify Equation (13) heating tests are carried out in small increments of about 2°C in the temperature ranges of the actual measurements. The rod is in stand still. The temperature change is thereby only caused by heat conduction and therefore requires a certain time to adjust itself. During the entrainment tests, the oil is moved through the rod and the temperature of the oil is assumed to be homogeneous. Therefore, conclusions can be drawn with the results of the heating tests on the temperature-induced volume increase during the entrainment tests.

Figure 8 shows the result of the heating test. The piston stroke of the entrainment sensor over the entire investigated temperature range would overstep the maximum stroke. Therefore, the piston is returned to the initial position for each measurement and only the relative changes are considered.

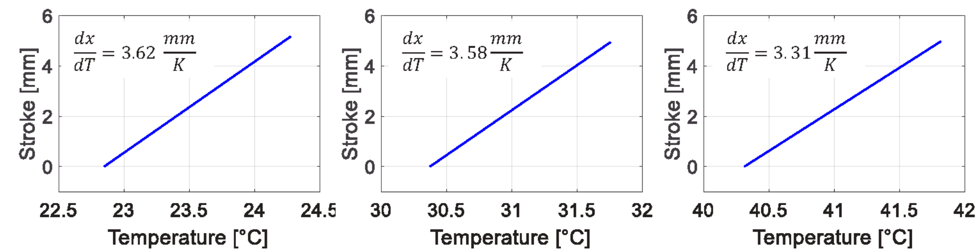

Figure 8: Temperature induced sensor displacement for different temperature ranges

It can be seen that the determined gradients deviate from the theoretical determined value. Reasons for this could be, for example, the non-linear expansion behavior of the sealing materials. Furthermore, the original oil volume can differ due to manufacturing inaccuracies. In addition, the expansion of the chamber itself can lead to a smaller gradient than determined before. As the last and most likely cause, it can be assumed that the heat coefficient used in the calculation differs from the actual.

The mean gradient determined is $3.50 \frac{mm}{K}$ with a standard deviation of 3.96%. This can be attributed to the resolution of the used sensors. The temperature sensors resolution is 0.1°K, which corresponds to an inaccuracy of 5% at a temperature range of around 2°C. The displacement measurement system, which measures the displacement of the piston, has a resolution of 0.075 mm, a further inaccuracy of 0.9% in the measured range. Overall accuracy therefore accounts to up to 5.9% as the errors are connected serially. The mean gradient was used to correct the influence of the temperature change during the entrainment measurements.

4 Entrainment Measurements

Subsequent, the results of the intake measurements are explained, which have been corrected for the temperature influence. Experiments are carried out with oil and with water separately, first oil and second water is used as test fluid. The pressure is 30 bar and the velocity of the rod 175 $\frac{mm}{s}$. In addition, the temperature is varied.

4.1.1 Measurement results

The raw travel signals of the piston displacement and the raw data of the temperature have discontinuities due to Stick-Slip of the entrainment sensor piston as well as due to discrete data increments of the temperature sensor and the used LVDT. Therefore, the measurement data for the displacement and the temperature were approximated by means of a second degree polynomial before the temperature compensation. Figure 8 shows the raw and the approximated signal for the temperature (left) and for the piston displacement (right).

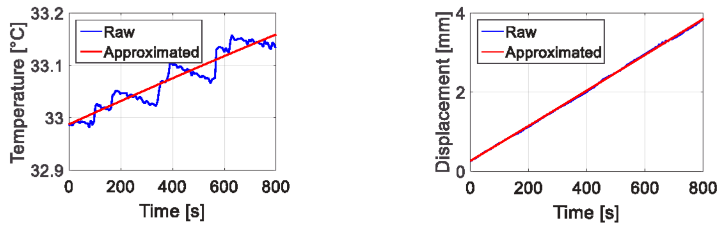

Figure 9: Raw data and approximated function, temperature left, displacement right

It is obvious, that there is good alignment between the approximated curve with the raw data of the displacement and a sufficient alignment of the temperature data. In the following, the approximated data is used for further calculations. A total of three measurement series are conducted for each measuring point. The data for each point is then approximated, temperature compensated and finally averaged.

Figure 10 shows the results of entrained fluid for different temperatures at a pressure of 30 bar. The red line represents the tests with oil as test fluid whereas the blue stands for water as test fluid.

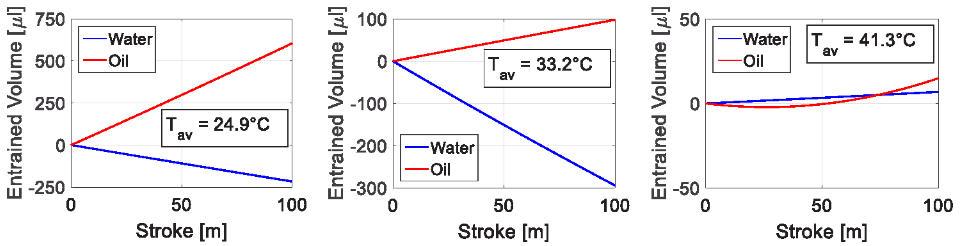

Figure 10: Entrainment of oil vs. water at different temperatures and 30 bar

Furthermore, the standard deviations of the averaged and compensated measurement series were calculated and are given in Table 2.

Temperature	Standard deviation Water	Standard deviation Oil
24.9°C	10.4%	10.6%
33.2°C	3.65%	1.47%
41.3°C	98.0%	91.8%

Table 2: Measurement standard deviations

For the highest temperature of 41.3°C, no significant entrainment could be measured, which simultaneously results in a very large standard deviation of the individual measuring series.

For the measurement at 24.9°C it can be seen that oil is dragged into the system. In the case of water, the entry is negative; meaning that fluid is discharged from the system. About 600 μl of oil are entrained over a total stroke of 100 m and some 200 μl is discharged when water is supplied.

At a temperature of 33.2°C, the intake curves are similar to the previous temperature. Approximately 100 μl of oil are drawn in over a stroke of 100 m whereas 300 μl are discharged when supplied with water.

4.1.2 Comparison and discussion of entrained fluid volume results

Linear ratios can be obtained for the linear entrainment curve at 24.9°C. and 33.2°C. This is not the case for the temperature of 41.3°C, since the draw-in equals zero. The average ratios are given in Table 3. The value of the theoretical ratio from Figure 3 is also given

Temperature	$\frac{\Delta V_{Water}}{\Delta V_{Oil}}$ measured	$\frac{\Delta V_{Water}}{\Delta V_{Oil}}$ theoretical
24.9°C	-0.366	0.108
33.2°C	-3.064	0.119

Table 3: Comparison of the measured and theoretical entrained volume ratios

It is clear that the ratios are very different from each other. Therefore, it can be assumed that the theory explained in chapter 2 is not applicable in the case of water entrainment.

A possible explanation for fluid volume exiting the chamber when external water is supplied may be that the oil film adhering to the rod during extension is detached in contact with water and rises due to the difference in density and is transported away from the sealing gap accordingly. The only lubricant then is water, which has a lower viscosity and is only slightly entrained back in. To ensure the measurement results other possibilities of rod-wetting will also be implemented and tested in the future.

5 Summary and conclusion

In this article, the water entrainment potential across piston rod seals in hydraulic cylinders was discussed.

First, the theory of Blok was applied to the case of water and necessary corrections for the viscosity were explained. Afterwards, the test bench was explained and the sensitivity and suitability were examined. Furthermore, the method for correcting the temperature change during the measurement was presented. Subsequently, the measurement results of the intake for oil and water were displayed and discussed. It was found that the measured intake volumes of water are negative over the stroke. In total, it was possible to measure entrainment of oil over a stroke length of 100 m of up to 600 μl and a loss of fluid volume in the chamber of up to 300 μl when suppling water at 30 bar chamber pressure.

It can be stated that the experimental results presented above do not correspond to that of the theoretical predictions. The most likely explanation is that the oil film attached to the rod is detached when contacted with water due to density differences. Water is then the only lubricant in the sealing gap which has a lower viscosity which leads to a smaller intake film height than the height during extension. Over all, fluid volume exits the chamber which has been measured.

6 Acknowledgements

The authors thank the Research Association for Fluid Power of the German Engineering Federation VDMA for its financial support. Special gratitude is expressed to the participating companies and their representatives in the accompanying industrial committee for their advisory and technical support.

Nomenclature

Variable	*Description*	*Unit*
A	Cross-sectional area	[mm²]
d	Rod diameter	[mm]
E'_{Fl}	Bulk modulus	[bar]
h	Gap height	[µm]
H	Stroke	[m]
p	Pressure	[bar]
Δp	Pressure difference	[bar]
T	Temperature	[°C]
u	Velocity	[mm/s]
V_0	Original volume	[m³]
ΔV	Entrained volume	[µl]
ΔV_i	Change of volume	[mm³]
Δx	Piston displacement	[mm]
θ	Change of temperature	[K]
η	Dynamic viscosity	[Pas]
γ	Expansion coefficient	[K^{-1}]

References

/1/ Rabinowicz, E., Lecture presented to the American Society of Lubricating Engineers, Bearing Workshop, USA, 1981

/2/ Boyde, S., *Green lubricants. Environmental benefits and impacts on lubrication*. Green Chemistry, 4, The Royal Society of Chemistry, 293-307, 2002

/3/ Totten, G., *Fuels and Lubricants Handbook: Technology, Properties, Performance, and Testing*, ASTM Manuel Series: MNL37WCD, ISBN 978-0803120969, 2003

/4/ Tumbrinck, M., *Der Einfluss von Wasser in mineralölbasischen Druckflüssigkeiten von Hydraulikanlagen*, Dissertation, RWTH Aachen, 1982

/5/ Blok, H., *Inverse Problems in Hydrodynamic Lubrication and Design Directives for Lubricated Flexible Surfaces*, Proc. Symp. On Lubrication and Wear, Houston USA, 1963

/6/ Haas, W. *Grundlehrgang Dichtungstechnik*, lecture notes, University Stuttgart, 2015.

/7/ Nißler, B. *Dichtheit von Hydraulikstangendichtringen aus Polyurethan*, Dissertation, University Stuttgart, 2015

/8/ Tao, J., *Untersuchung der physikalischen Vorgänge im Dichtspalt und des Reibungsverhaltens von Hydraulik-Stangendichtungen*, Dissertation, RWTH Aachen University, 1991

/9/ Murrenhoff, H., *Fundamentals of Fluid Power Technology – Vol.1: Hydraulics*, lecture notes, RWTH Aachen, 2016